Spatial Correlation between Hyperpigmentary Changes on Color Fundus Photography and Hyperreflective Foci on SDOCT in Intermediate AMD

Francisco A. Folgar,[1,7] *Jessica H. Chow,*[1,7] *Sina Farsiu,*[1,2] *Wai T. Wong,*[3] *Stefanie G. Schuman,*[1] *Rachelle V. O'Connell,*[1] *Katrina P. Winter,*[1] *Emily Y. Chew,*[3] *Thomas S. Hwang,*[4] *Sunil K. Srivastava,*[5] *Molly W. Harrington,*[6] *Traci E. Clemons,*[6] *and Cynthia A. Toth*[1,2]

Purpose. Macular hyperpigmentation is associated with progression from intermediate to advanced age-related macular degeneration (AMD). The purpose of this study was to accurately correlate hyperpigmentary changes with spectral domain optical coherence tomography (SDOCT) hyperreflective foci in eyes with non-advanced AMD.

Methods. A prospective cross-sectional analysis of 314 eyes (314 subjects) with intermediate AMD was performed in the multicenter Age-Related Eye Disease Study 2 (AREDS2) Ancillary SDOCT Study to correlate hyperpigmentary changes on color fundus photographs (CFP) with abnormal morphology on SDOCT. Spatial coregistration was performed with an automated algorithm in two nonoverlapping subsets of 20 study eyes, which permitted double-masked CFP and SDOCT grading by certified investigators.

Results. Macular CFP hyperpigmentation was significantly associated with SDOCT intraretinal hyperreflective foci in the 314 study eyes ($P < 0.001$). In a substudy of 40 eyes, automated intermodality spatial coregistration was successfully achieved in all 136 (100%) retinal regions selected for CFP and SDOCT grading. In one subset of 20 study eyes, 28 of 39 (71.8%) retinal CFP regions with hyperpigmentation were correlated with focal hyperreflectivity on SDOCT, versus seven of 39 (17.9%) control regions ($P < 0.001$). In another subset of 20 eyes, 21 of 29 (72.4%) SDOCT regions with hyperreflective foci were correlated with hyperpigmentary changes on CFP, versus two of 29 (6.9%) control regions ($P < 0.001$).

Conclusions. A novel algorithm achieves automated intermodality spatial coregistration for masked grading of regions selected on CFP and SDOCT. In intermediate AMD, macular hyperpigmentation has high spatial correlation to SDOCT hyperreflective foci and often represents the same anatomical lesion. (ClinicalTrials.gov number, NCT00734487.) (*Invest Ophthalmol Vis Sci.* 2012;53:4626–4633) DOI: 10.1167/iovs.12-9813

Age-related macular degeneration (AMD) is a staged disease that progresses from early and intermediate stages characterized by drusen and pigmentary changes, to advanced stages characterized by choroidal neovascularization (CNV) or central geographic atrophy (GA).[1–7] Pigmentary changes in the macula are a defining feature of intermediate AMD.[8–13] Pigmentary changes appear on clinical examination or color fundus photography either as hypopigmentary changes, which are seen as depigmented areas of the retinal pigment epithelium (RPE) not meeting criteria for GA, or hyperpigmentary changes, which are deposits of gray or black pigment within the retina or at the level of the RPE.[12,13]

Numerous epidemiologic and interventional studies have demonstrated that the presence of macular pigmentary changes in intermediate AMD increases the risk of progression to both forms of advanced AMD—CNV and central GA.[7,11–13] The Complications of AMD Prevention Trial (CAPT) found that focal hyperpigmentation was a risk factor for both the development of CNV and central GA, while RPE depigmentation was significantly associated with central GA only.[14] These associations support the theory that pigmentary changes are pathologic abnormalities related to the mechanisms driving AMD progression.

Currently, focal hyperpigmentation in intermediate AMD is presumed to result from RPE displacement, migration, or degeneration, but correlative histopathologic studies have not yet been performed.[15–17] Evaluation of pigmentary changes in major clinical trials has historically relied on 2-dimensional color fundus photography (CFP); however, optical coherence tomography (OCT) offers a 3-dimensional cross-sectional view of this retinal pathology.

Spectral-domain OCT (SDOCT) improves the characterization of AMD pathology, including photoreceptor and RPE damage, drusen ultrastructure, and geographic atrophy.[18,19] Leuschen et al.[20] have described the SDOCT characteristics of retinal pathology in a large cross-sectional study of patients with category 3 AMD enrolled in a multicenter randomized

From the [1]Duke University Eye Center and the [2]Department of Biomedical Engineering, Duke University, Durham, North Carolina; [3]National Eye Institute, National Institutes of Health, Bethesda, Maryland; [4]Devers Eye Institute, Portland, Oregon; [5]Cole Eye Institute, Cleveland Clinic, Cleveland, Ohio; and [6]The EMMES Corporation, Rockville, Maryland.

[7]These authors contributed equally to the work presented here and should therefore be regarded as equivalent authors.

Presented in part at the annual meeting of the American Academy of Ophthalmology, Chicago, Illinois, October 2010.

Supported by the AREDS2 Ancillary SDOCT Study (ClinicalTrials.gov identifier: NCT00734487), the American Health Assistance Foundation (SF), and Research to Prevent Blindness (SF). The AREDS2 Grant is supported in part by Bioptigen (equipment), Genentech (IST-4400S grant), and Alcon Laboratories (unrestricted grant).

Submitted for publication March 7, 2012; revised May 1, 2012; accepted May 2, 2012.

Disclosure: **F.A. Folgar**, None; **J.H. Chow**, None; **S. Farsiu**, P; **W.T. Wong**, ARVO/IOVS (S); **S.G. Schuman**, None; **R.V. O'Connell**, None; **K.P. Winter**, None; **E.Y. Chew**, ARVO/IOVS (S); **T.S. Hwang**, None; **S.K. Srivastava**, None; **M.W. Harrington**, None; **T.E. Clemons**, None; **C.A. Toth**, Bioptigen (F), Genentech (F), Alcon (F), Physical Sciences Inc (C), P

Corresponding author: Cynthia A. Toth, Duke University Eye Center, DUMC 3802, Durham, NC 27710; cynthia.toth@duke.edu.

clinical trial, and Jain et al.[21] quantitatively correlated drusen size on CFP to drusen segmented on SDOCT from the same clinical trial. Ho et al.[22] recently reported the results of a single-center study that correlated intraretinal pigment migration on high-resolution OCT with RPE pigment clumping on fundus photographs using cross-modality image registration. The authors manually overlapped OCT-derived retinal images over CFP to show that hyperreflective pigment migration on untracked OCT scans coincided with CFP hyperpigmentation in all 30 eyes with AMD.[22] A one-or-none system for detecting pathology was performed by unmasked investigators who simultaneously examined both CFP and OCT. The nearly perfect agreement between imaging modalities was reported without objective spatial correlation of the observed lesions. Sites of macular hyperpigmentation were not evaluated for other OCT features, and so it still remains unclear if macular hyperpigmentation in AMD represents a single or diverse set of pathologic processes.

In intermediate AMD, hyperreflective foci on SDOCT are defined as lesions of equal or higher reflectivity than the RPE band, located within the neurosensory retina, often discrete and well-circumscribed, but sometimes seen attached to elevated RPE overlying drusen.[22] The purpose of the present study was to use an automated algorithm to perform precise double-masked spatial comparison of CFP hyperpigmentation with SDOCT hyperreflective foci in eyes with category 3 AMD currently enrolled in the Age-Related Eye Disease Study 2 (AREDS2).

Methods

Patient Population

The AREDS2 Ancillary SDOCT Study (ClinicalTrials.gov identifier NCT00734487) is an ancillary study to the prospective multicenter randomized AREDS2 (ClinicalTrials.gov identifier NCT00345176). Major inclusion and exclusion criteria for AREDS2 have been previously described.[23] The purpose of the SDOCT Ancillary Study was to identify whether changes in AMD over time, as seen with SDOCT, can be used to predict vision loss and the advancement of AMD in people at moderate-to-high risk for progression. Details of the design and methods, the protocol for scoring SDOCT volumes by certified SDOCT readers, and a description of the baseline characteristics of the participants have been previously reported.[20] The study protocol was approved by the institutional review board associated with each center and followed the tenets set forth by the Declaration of Helsinki. Written informed consent was obtained from each participant, and data management was compliant with guidelines from the Health Insurance Portability and Accountability Act.

Enrollment and Designation of Study Eyes

There were 314 participants, recruited from four AREDS2 clinical trial centers in the United States, who were identified to have category 3 AMD in at least one eye based on CFP grading criteria. Each participant was consented to enroll in the AREDS2 Ancillary SDOCT Study and contributed only one eye with category 3 AMD to the analysis of the current study. For patients with bilateral category 3 AMD, the right eye was arbitrarily designated as the study eye. Baseline CFP and SDOCT were obtained for all 314 study eyes at their respective clinical centers.

Image Acquisition and Grading for CFP and SDOCT

Color fundus photographs were taken by certified ophthalmic photographers at the baseline visit for each subject, following a standard AREDS2 fundus photography protocol, with 35-degree stereoscopic fundus cameras (Zeiss FF450^{plus}; Carl Zeiss Meditec, Dublin, CA) or (Topcon 50-XT; Topcon Medical Systems, Oakland, NJ).[23] Digital photographs were imported to a computer imaging system (Zeiss Visupac; Carl Zeiss Meditec) or (Topcon IMAGEnet R4; Topcon Medical Systems).[23] All photographs were graded by certified readers at the Wisconsin Fundus Photograph Reading Center (University of Wisconsin, Madison, WI) according to the AREDS grading system, which included scoring for the presence or absence of focal hyperpigmentary changes.[24] The CFP grading results were obtained from the AREDS2 Coordinating Center (The EMMES Corporation, Rockville, MD).

OCT images were captured by certified technicians at the baseline visit for each subject, following a set protocol for AREDS2 SDOCT imaging with a spectral-domain ophthalmic imaging system (Bioptigen SDOIS; Bioptigen, Research Triangle Park, NC). The SDOCT volume scans in this study were obtained with an 840-nm wavelength superluminescent diode light source, covering a 6.7-mm $\times$ 6.7-mm area centered on the fovea, and consisting of 100 horizontal B-scan lines with 1000 A-scans per line. B-scans were obtained at an interval of 66 μm between lines and achieved an axial resolution of 4.5 μm. The baseline SDOCT volumetric scans for all study eyes were graded for the presence or absence of focal intraretinal hyperreflectivity signals by an AREDS2 Ancillary SDOCT Study-certified reader at the Duke Advanced Research in SDOCT Imaging Laboratory (DARSI, Duke University, Durham, NC). The presence or absence of these SDOCT features was compared with the presence or absence of focal hyperpigmentary changes on CFP for all 314 study eyes by masked investigators at the AREDS2 Coordinating Center.

Spatial Correlation between Hyperpigmentary Changes and Hyperreflective Signals

Two nonoverlapping subsets of 20 study eyes were selected for a double-masked spatial correlation of CFP hyperpigmentary changes with SDOCT intraretinal hyperreflectivity signals. These subsets were designated Group A and Group B.

Group A comprised 20 eyes that were randomly selected from AREDS2 Ancillary SDOCT Study eyes that were previously graded by the Wisconsin Fundus Photograph Reading Center as containing focal hyperpigmentation, and which met the following criteria: (1) at least one site of macular hyperpigmentation within two disc diameters from the center of the fovea as determined by two independent CFP readers, and (2) no significant media opacity on CFP that would obscure the precise localization of hyperpigmentation or retinal vasculature.

Group B comprised 20 eyes that were randomly selected from the enrolled eyes that were scored at the DARSI Laboratory as containing hyperreflective foci on SDOCT, and which met the following criteria: (1) at least one focal site of hyperreflectivity within two disc diameters of the center of the fovea as determined by two independent SDOCT readers, (2) adequate visualization of retinal vasculature en face to permit for alignment of the scan to the corresponding CFP, (3) no scan volume distortions secondary to patient motion artifact, and (4) sufficient image quality to allow clear visualization of SDOCT features as determined by certified readers. The summed voxel projection (SVP) derived from SDOCT volume scans and the corresponding CFP were spatially aligned using retinal vasculature as landmarks for orientation and registration using imaging software (Adobe Photoshop CS4; Adobe Systems, San Jose, CA).

Regions of interest (ROIs) were defined to guide the cross-modality correlation analyses. Each ROI was defined as a 333-μm $\times$ 333-μm area entirely contained within two disc diameters from the center of the fovea. The 333-μm vertical dimension comprised five horizontal B-scan lines spaced 66 μm apart on SDOCT.

In Group A, the boundaries of *hyperpigmentation* ROIs were positioned on the CFP image, such that each ROI entirely encompassed an area of hyperpigmentation. Up to two separate nonoverlapping *hyperpigmentation* ROIs were defined for each eye in Group A (only one ROI was selected in eyes that had only one site of hyperpigmentary change). For each *hyperpigmentation* ROI, a *control* ROI was

identified in a nearby retinal area containing a similar retinal background but lacking any area of hyperpigmentary change. The selection and placement of Group A ROIs were performed by an experienced retinal physician (SGS) masked to SDOCT grading. On the corresponding SDOCT scans, all ROIs in Group A were graded for abnormal OCT features by a certified reader masked to CFP images.

In Group B, focal hyperreflectivity overlying the RPE was identified on SDOCT, and an ROI was centered over this lesion. Up to two *focal hyperreflectivity* ROIs were identified on SDOCT volume scans for each eye (only one ROI was selected in eyes that had only one hyperreflective lesion). For each defined *focal hyperreflectivity* ROI, a *control* ROI that lacked any focal hyperreflective changes was randomly identified on the same SDOCT scan. The selection of Group B ROIs was performed by a certified AREDS2 Ancillary SDOCT Study reader (KPW) masked to CFP grading. On corresponding CFP scans, all ROIs in Group B were graded for pigmentary changes by a retinal physician masked to SDOCT images.

Based on the Duke OCT Retinal Analysis Program (DOCTRAP) software platform described elsewhere,[25,26] a customized algorithm was developed with technical programming software (MATLAB; MathWorks, Natwick, MA), which displayed SDOCT volume scans aligned with their SVP and corresponding CFP. The software's graphic user interface was designed to keep CFP images masked while the corresponding SDOCT ROIs were viewed and graded, and vice versa (Fig. 1). The certified SDOCT reader, masked to CFP viewing, evaluated all SDOCT ROIs from Groups A and B for the presence or absence of each of the SDOCT findings listed in Table 1. The retinal physician evaluated all CFP ROIs from Groups A and B for the presence or absence of each of the CFP findings listed in Table 1, while remaining masked to SDOCT images. On all photographs, depigmented RPE changes were graded the same as RPE atrophy.

Statistical Analysis

Correlations between occurrence of focal hyperpigmentary changes on CFP and intraretinal hyperreflectivity foci on SDOCT were calculated with the Pearson χ^2 test. The Group A prevalence of hyperreflectivity among study eyes with CFP hyperpigmentation and, conversely, the Group B prevalence of focal hyperpigmentation among study eyes with SDOCT hyperreflective foci were calculated by applying a generalized linear model procedure (GENMOD) with a binomial probability distribution and specifying a repeated statement to account for correlation between any ROIs from the same eye. All CFP and SDOCT images from the spatial correlation substudy were graded again by separate masked readers, and reproducibility was expressed as the interreader agreement percentile, the Cohen κ coefficient, and its standard error. All statistical analysis was performed using analytics software (SAS 9.2; SAS Institute Inc, Cary, NC).

Results

Intermodality CFP-SDOCT Association without Detailed Spatial Correlation

Out of the 314 category 3 AMD study eyes, 239 (76.1%) eyes had hyperpigmentary changes on CFP grading by the Wisconsin Fundus Photograph Reading Center, and 175 (55.7%) eyes had at least one focal site of hyperreflectivity on SDOCT (Table 2). There was a statistically significant correlation between the presence of CFP hyperpigmentation and SDOCT hyperreflectivity ($P < 0.001$, 2-tailed Fisher exact test) with an agreement of 69.4% ($n = 218$) on the presence or absence of hyperpigmentation on CFP and focal hyperreflectivity on SDOCT, and 30.6% ($n = 96$) disagreement between modalities (Table 2).

Table 1. SDOCT and CFP Variables Graded for Each ROI in Groups A and B

SDOCT Variables

1. Focal hyperreflectivity:
   a. Intraretinal location above RPE:
      i. Photoreceptor OS (at or below IS band)
      i. Photoreceptor layer (above IS band)
      iii. Hyperreflective aspect of outer plexiform layer
      iv. Inner nuclear layer
      v. Above inner nuclear layer
   b. Focal hyperreflectivity at apex of drusen
   c. With photoreceptor layer thinning
   d. With OS loss/shortening
2. Drusen
   a. Foveal: center of region $\leq$500 μm from center of the fovea
   b. Core: RPE elevation with distinct internal focus of hyperreflectivity or hyporeflectivity
      i. Hyperreflective core: relative to surrounding sub-RPE material
      ii. Hyporeflective core: relative to surrounding sub-RPE material
   c. Internal reflectivity: predominant reflectivity of sub-RPE material*
      i. Low: $\leq$ reflectivity of PRL
      ii. Medium: $>$ reflectivity of PRL and $<$ reflectivity of RPE
      iii. High: $\geq$ reflectivity of RPE
3. RPE atrophy
4. Normal RPE: no evidence of RPE elevation or atrophy in the region

CFP Variables

1. Focal hyperpigmentation
   a. Foveal: center of region $\leq$500 μm from center of the fovea
   b. With drusen
   c. With RPE atrophy
   d. Largest longitudinal diameter of hyperpigmentation (μm)
2. Drusen
   a. Hard/Crystalline
   b. Soft
3. RPE atrophy
4. Normal RPE: no evidence of drusen or RPE atrophy in the region

OS, outer segment; IS, inner segment; PRL, photoreceptor layer.
* Classification described by Leuschen et al.[20]

Group A: Spatial Correlation of Hyperpigmentation Identified on CFP to Pathology on SDOCT

A total of 78 ROIs (39 *hyperpigmentary* and *control* ROIs) were defined on CFP in the 20 eyes enrolled in Group A. Automated spatial correlation to SDOCT and masked grading of both imaging modalities were successfully achieved for all 78 (100%) regions.

The results of SDOCT grading for Group A are presented in Table 3. In this investigation's primary study endpoint, 28 of 39 (71.8%) *hyperpigmentary* ROIs in Group A contained focal hyperreflectivity either within the retina (Fig. 2A) or within the inner aspect of the RPE over drusen (Fig. 2B), compared with seven (17.9%) *control* ROIs ($P < 0.001$). Intraretinal SDOCT hyperreflectivity was detected in 15 (38.5%) *hyperpigmentary* ROIs, compared with three (8.1%) *control* ROIs ($P = 0.002$); while the prevalence of focal hyperreflectivity at the inner aspect of the RPE/drusen complex was detected in 20 (51.3%) *hyperpigmentary* ROIs, versus only four (10.8%) *control* ROIs ($P < 0.001$).

Table 2. Intermodality CFP-SDOCT Association without Spatial Correlation, Expressed as Number of Eyes (Percentile), for One Eye from Each Subject Enrolled in the AREDS2 Ancillary SDOCT Study ($n = 314$ eyes)

CFP Hyperpigmentation	SDOCT Hyperreflective Foci		
	Yes	No	Total
Yes	159 (50.6%)	80 (25.5%)	239 (76.1%)
No	16 (5.1%)	59 (18.8%)	75 (23.9%)
Total	175 (55.7%)	139 (44.3%)	314

In terms of axial retinal localization, the majority of *hyperpigmentary* ROIs had SDOCT hyperreflective foci adjacent to the inner aspect of drusen (51.3%), followed by the outer nuclear layer (35.9%), outer plexiform layer (10.3%), photoreceptor outer segments (5.1%), and finally the fewest regions had foci in the inner nuclear layer (2.6%, Fig. 3). Focal hyperreflectivity was not found in retinal layers internal to the inner nuclear layer. Intraretinal hyperreflective foci were associated with photoreceptor layer thinning in nine (23.1%) *hyperpigmentary* ROIs and with photoreceptor outer segment loss in 12 (30.8%) of these regions ($P = 0.014$ and $P = 0.007$, respectively, versus *control* ROIs).

In a post hoc analysis, the authors reviewed the 11 regions (28.2%) without hyperreflective foci on SDOCT, and the reviewers confirmed the lack of foci as initially determined by certified readers. Five of these regions had drusen with homogenous sub-RPE hyperreflectivity. Two regions had drusen with medium reflectivity and a hyperreflective core. Four regions had foci of medium reflectivity (between outer nuclear layer and RPE band reflectivity) attached to drusen apices, which did not meet the predetermined criteria for hyperreflectivity.

In contrast to CFP grading, RPE atrophy was only detected on SDOCT in two *hyperpigmentary* ROIs by certified readers, which was statistically similar to *control* ROIs (Table 3). In another post hoc analysis, the authors reviewed the six hyperpigmentary regions in Group A with concurrent RPE atrophy graded on CFP but not on SDOCT. All six regions contained areas of CFP hypopigmentation that were spatially correlated on SDOCT to small drusen with medium reflectivity, overlying outer nuclear layer thinning, and no foci of hyperreflectivity.

The results of CFP grading of these ROIs are presented in Table 4. There was no significant difference in drusen characteristics on CFP between *hyperpigmentary* ROIs and *control* ROIs; however, RPE atrophy on CFP was more prevalent in *hyperpigmentary* ROIs (8 vs. 1, respectively, $P = 0.03$), while normal RPE without associated AMD pathology was more prevalent in *control* ROIs (12 vs. 0, respectively, $P < 0.001$).

Group B: Spatial Correlation of Focal Hyperreflectivity Identified on SDOCT to Other Findings of SDOCT and to Pathology on CFP

A total of 58 ROIs (29 *focal hyperreflectivity* and *control* ROIs) were defined on SDOCT in the 20 eyes enrolled in Group B. Automated spatial correlation to CFP and masked grading of both imaging modalities were successfully achieved for all 58 (100%) regions.

The results of CFP grading for the ROIs in Group B are presented in Table 4. In this investigation's primary study endpoint, CFP hyperpigmentation was present in 21 out of 29 (72.4%) SDOCT *hyperreflectivity* ROIs (Fig. 2C), compared with two out of 29 (6.9%) SDOCT *control* ROIs ($P < 0.001$, Table 4). Of note, *focal hyperreflectivity* ROIs were more likely to be located within a 500-μm radius of the center of the fovea, as opposed to *control* ROIs, which were more often further away from the foveal center (27.6% vs. 3.4%, respectively, $P = 0.03$, Table 4). On CFP grading, there was no significant difference in drusen characteristics, prevalence of RPE atrophy, or hyperpigmentation size between the two ROI categories.

The results of SDOCT grading for Group B are presented in Table 3. As expected, *focal hyperreflectivity* ROIs had a

Table 3. Spatial Correlation of SDOCT Findings within ROIs for Group A (Hyperpigmentary versus Control Regions on CFP) and Group B (Hyperreflectivity versus Control Regions on SDOCT), Expressed as Number of Regions (Percentile)

SDOCT Findings	Frequency in Group A (20 Eyes)			Frequency in Group B (20 Eyes)		
	CFP Hyperpigmentary Regions ($n = 39$)	CFP Control Regions ($n = 39$)	*P* Value*	SDOCT Hyperreflectivity Regions ($n = 29$)	SDOCT Control Regions ($n = 29$)	*P* Value*
1. Hyperreflective foci†	28 (71.8%)	7 (17.9%)	<0.001	29 (100%)	2 (6.9%)	<0.001
a. Intraretinal hyperreflectivity	15 (38.5%)	3 (8.1%)	0.002	29 (100%)	0	<0.001
b. Hyperreflectivity at the apex of drusen	20 (51.3%)	4 (10.3%)	<0.001	8 (27.6%)	2 (6.9%)	0.04
c. With photoreceptor layer thinning	9 (23.1%)	1 (2.6%)	0.014	13 (44.8%)	0	<0.001
d. With OS loss/shortening	12 (30.8%)	2 (5.1%)	0.007	18 (62.1%)	0	<0.001
2. Drusen	33 (84.6%)	27 (69.2%)	0.18	28 (96.6%)	24 (82.8%)	0.19
a. Foveal	22 (56.4%)	1 (2.6%)	<0.001	9 (31.0%)	5 (17.2%)	0.36
b. Core						
Hyperreflective	1 (2.6%)	1 (2.6%)	1.0	0	0	–
Hyporeflective	0	0	–	0	0	–
c. Internal reflectivity						
Low	1 (2.6%)	0	1.0	1 (3.4%)	1 (3.4%)	1.0
Medium	34 (87.2%)	24 (61.5%)	0.03	27 (93.1%)	24 (82.8%)	0.19
High	13 (33.3%)	9 (23.1%)	0.45	8 (27.6%)	5 (17.2%)	0.53
3. RPE atrophy	2 (5.1%)	1 (2.6%)	1.0	1 (3.4%)	3 (10.3%)	0.61
4. Normal RPE	4 (10.3%)	22 (56.4%)	<0.001	8 (27.6%)	6 (20.7%)	0.76

* Fisher exact test.

† Some regions contain >1 focal hyperreflective lesion.

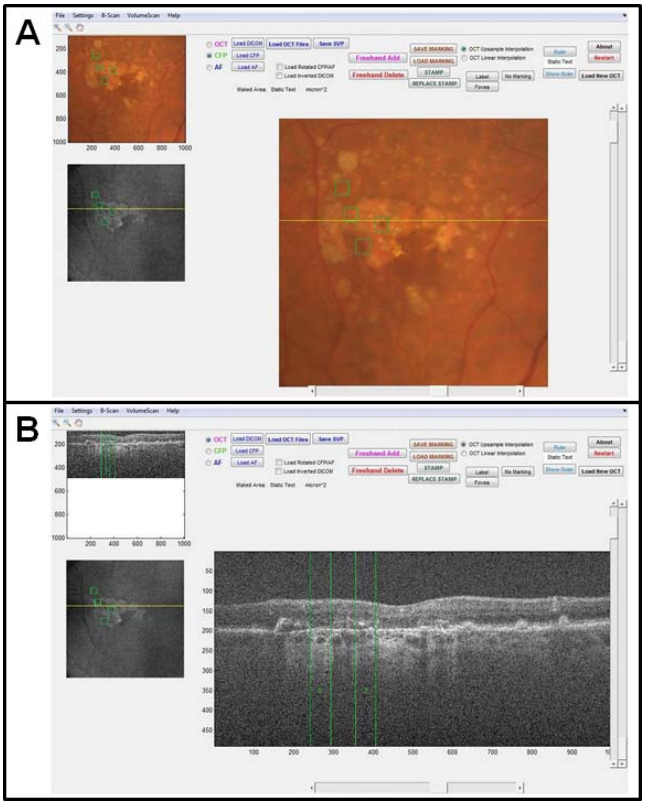

Figure 1. Graphic user interface of the proprietary software developed at the Duke University Eye Center (Durham, NC) that was used to perform spatial correlation and grading for each ROI. (**A**) Hyperpigmentary changes on CFP were identified with green marks (*top left*). The SVP, derived from an SDOCT scan volume (*bottom left*), underwent coregistration with CFP (*center*). (**B**) Marks from the SVP (*bottom left*) were projected onto the SDOCT scans as green axial lines marking the boundaries of the 333 × 333-μm square ROI centered on each SVP mark (*top left*). The SDOCT scan shown here (*center*), corresponding to the yellow line on CFP and SVP, was graded for the presence of hyperreflective foci and associated pathology within the marked boundaries of two ROIs.

significantly greater prevalence of intraretinal hyperreflectivity on SDOCT grading, as well as associated photoreceptor layer thinning and outer segment loss, compared with *control* ROIs without intraretinal hyperreflectivity ($P < 0.001$ for all three variables, Table 3). Foci attached to the inner aspect of drusen were present in eight out of 29 (27.6%) *focal hyperreflectivity* ROIs, versus two out of 29 (6.9%) *control* ROIs ($P = 0.04$, Table 3) on SDOCT.

In terms of axial retinal localization, the majority of *focal hyperreflectivity* ROIs had hyperreflective foci in the outer nuclear layer (96.6%), followed by the outer plexiform layer (37.9%), the inner nuclear layer (37.9%), the inner aspect of drusen (27.6%), and then zero regions with foci detected in the photoreceptor outer segments. On SDOCT grading, there was no statistical difference in drusen characteristics or the prevalence of RPE atrophy for *focal hyperreflectivity* versus *control* ROIs (Table 3).

Reader reproducibility for each imaging modality in the spatial correlation substudy was superior to the cross-modality variability between SDOCT and CFP. There was 85.5% reader agreement for SDOCT hyperreflectivity (Cohen κ 0.69, SE 0.18) and 95.7% reader agreement for CFP hyperpigmentation (Cohen κ 0.91, SE 0.03).

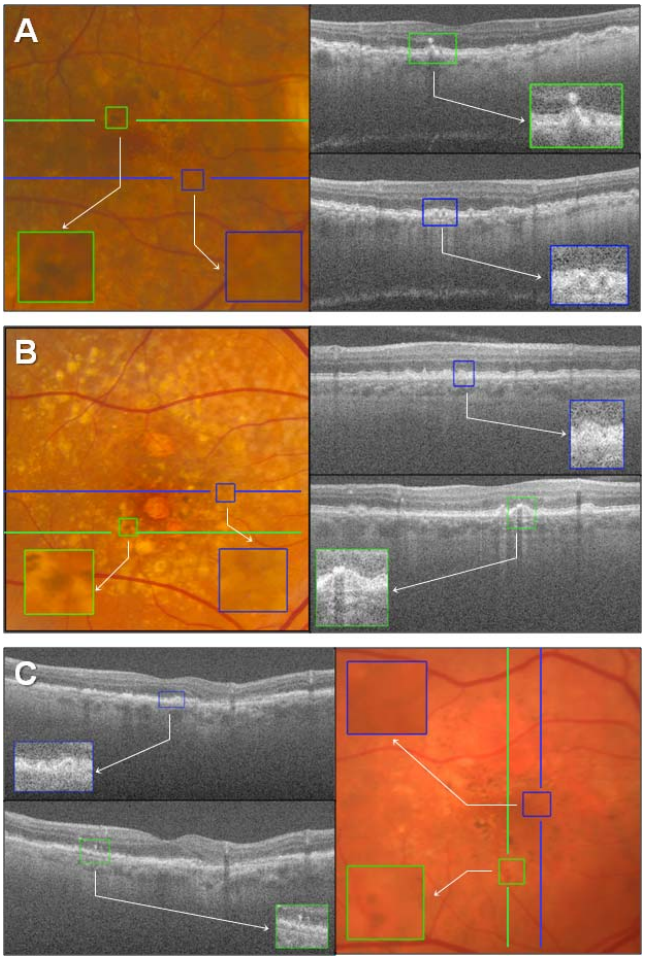

Figure 2. Examples of spatially CFP hyperpigmentation, SDOCT hyperreflective foci, and control regions. (**A**) Hyperpigmentation on CFP corresponds to hyperreflectivity within the retina (*green*) on SDOCT, versus control region without CFP hyperpigmentation (*blue*). (**B**) CFP hyperpigmentation corresponds to SDOCT hyperreflectivity at the inner RPE on the apex of drusen (*green*), versus control region without CFP hyperpigmentation (*blue*). (**C**) SDOCT hyperreflectivity in the retina corresponds to CFP hyperpigmentation (*green*), versus control region without SDOCT hyperreflectivity (*blue*).

Discussion

This study has presented a method of automated image coregistration that allowed precise spatial correlation and double-masked grading for CFP and SDOCT imaging. Hyperpigmentation on CFP was significantly correlated with the focal hyperreflective lesions on SDOCT in eyes with intermediate AMD. The results of spatial correspondence showed that the spatial location of these two intermodal features was often correlated at the same site in the same eye, and therefore these features often represented the same anatomical lesion.

Hyperreflective foci were detected on SDOCT primarily at the apex of drusen or within the photoreceptor layer of the retina. Hyperreflective foci above drusen were previously noted on SDOCT imaging of eyes with nonadvanced AMD, and were anatomically associated with focal pigment migration on high-resolution OCT.[22,27] This study's quantitative survey revealed that most hyperpigmentary changes were associated with hyperreflectivity located at the inner border (apex) of drusen (Figs. 2B, 3), a previously unreported finding.

This quantitative correlation between hyperpigmentation and hyperreflective foci differed from the correlation reported

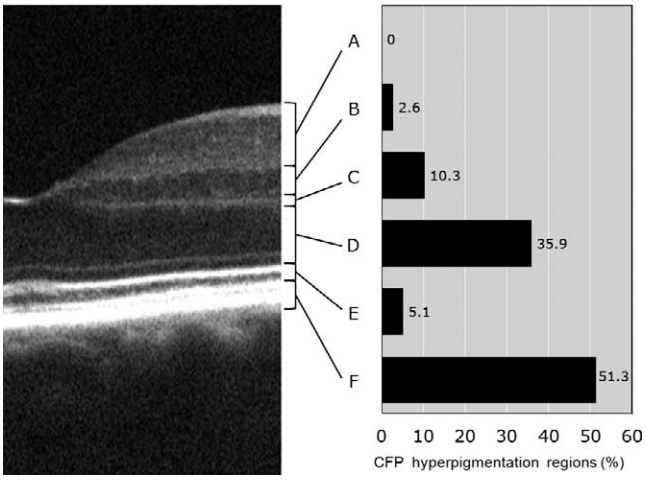

Figure 3. Distribution of Group A hyperpigmentation regions with respect to retinal localization of SDOCT hyperreflective foci. Retinal localization of corresponding SDOCT hyperreflectivity was scored for each ROI according to six axial retinal zones (**A**–**F**). Ten of 39 regions had foci in more than one zone. There were no regions with hyperreflectivity above the inner nuclear layer (**A**), one (2.6%) in the inner nuclear layer (**B**), four (10.3%) in the outer plexiform layer (**C**), 14 (35.9%) in the outer nuclear or photoreceptor layer (**D**), two (5.1%) in the photoreceptor outer segments (**E**), and 20 (51.3%) regions had foci at the inner RPE/druse apex (**F**).

by Ho et al.,[22] in which 30 of 31 (96.8%) eyes with pigment clumping on CFP exhibited intraretinal focal hyperreflectivity on SDOCT from the same visit. This discrepancy was likely due to different methods of imaging correlation. Ho et al.[22] recognized that the use of untracked SDOCT scans made it impossible to achieve exact registration of SDOCT to CFP. Selection bias may have been present in their study when SDOCT B-scans were graded and matched to CFP by unmasked investigators. In the present study, CFP were spatially aligned with vascular landmarks to the SVP retinal image, underwent automated SDOCT coregistration, and were evaluated for pathology in masked fashion.

Despite a statistically significant intermodality spatial correlation, a correlation between pigment on CFP and hyperreflectivity on SDOCT was only found in 71.8% of regions containing focal hyperpigmentation. In Group A, 28.2% of hyperpigmentation regions did not have corresponding hyperreflective foci on SDOCT. There are a number of potential reasons why a complete correlation was not found.

First, despite the increased resolution of SDOCT imaging compared with time-domain OCT, over 50% of the physical volume of the retina was not captured by the SDOCT raster scan algorithm. Individual B-scans for each SDOCT volume were acquired at 66-μm intervals. Assuming a width of 15 to 20 μm sampled by the SDOCT beam at the retina between B-scans, approximately 46 to 51 μm of intervening space remained unsampled. The authors theorize that small hyperreflective foci may have been present within these unscanned regions and so remained undetected. This also explains why the diameter and area measurements of hyperreflective foci could not be accurately compared with CFP measurements in the present study's protocol. Although hyperpigmentation area may be estimated with the high resolution provided by digital CFP, the unsampled space between SDOCT raster scan lines can result in significant underestimation of the diameter and area of hyperreflective foci. Forthcoming SDOCT segmentation algorithms and faster scanning technology will enable higher resolution of these lesions and accurate correlation of area measurements.

Second, it is likely that focal hyperpigmentation in intermediate AMD does not always correspond with hyperreflective foci on SDOCT. In the post hoc analysis, the authors reviewed the 11 regions without hyperreflective foci and identified specific SDOCT changes that did not meet the criteria for hyperreflectivity. They may represent RPE hypertrophy, hyperpigmentation of the choroid or sub-RPE space, or low-reflective RPE changes at the apex of drusen that manifest as CFP hyperpigmentation prior to developing SDOCT hyperreflectivity.

Similarly, in the second spatial correlation study evaluating Group B eyes, 72.4% of SDOCT regions containing focal intraretinal hyperreflectivity had corresponding hyperpigmentation on CFP (Table 3). Although this association was significantly greater compared with SDOCT *control* regions, the lack of total agreement may have been a result of a variable appearance of hyperreflective foci on CFP, some of which may not resemble hyperpigmentation. In prior reports, hyperreflective foci above drusen on SDOCT have been theorized to correspond to an abnormal deposit of varied etiologies such as extracellular pigment, migrated RPE cells, pigment-laden macrophages, lipid exudates, calcification, intraretinal hemor-

Table 4. Spatial Correlation of Photographic Findings within ROIs for Group A (Hyperpigmentary Regions versus Control Regions) and Group B (Hyperreflectivity Regions versus Control Regions), Expressed as Number of Regions (Percentile)

	Frequency in Group A (20 Eyes)			Frequency in Group B (20 Eyes)		
Photographic Findings	**CFP Hyperpigmentary Regions (n = 39)**	**CFP Control Regions (n = 39)**	***P* Value***	**SDOCT Hyperreflectivity Regions (n = 29)**	**SDOCT Control Regions (n = 29)**	***P* Value***
1. Focal hyperpigmentation	39 (100%)	0	<0.001	21 (72.4%)	2 (6.9%)	<0.001
a. Foveal	21 (53.8%)	0	<0.001	8 (27.6%)	1 (3.4%)	0.03
b. With drusen	*Under CFP grading (2) drusen*			19 (65.5%)	2 (6.9%)	<0.001
c. With RPE atrophy	*Under CFP grading (3) RPE atrophy*			1 (3.4%)	0	1.0
d. Diameter mean ± SD (μm)	232 ± 139	–	–	178 ± 121	124 ± 104	0.59
2. Drusen	33 (84.6%)	27 (69.2%)	0.18	25 (86.2%)	26 (89.6%)	1.0
a. Hard/Crystalline	3 (7.7%)	1 (2.6%)	0.62	0	1 (3.4%)	1.0
b. Soft	31 (79.5%)	27 (69.2%)	0.44	25 (86.2%)	25 (86.2%)	1.0
3. RPE atrophy	8 (20.5%)	1 (2.6%)	0.03	1 (3.4%)	2 (6.9%)	1.0
4. Normal RPE	0	12 (30.8%)	<0.001	2 (6.9%)	1 (3.4%)	0.61

* Fisher exact test, except for (1d) *P* value by the Mann-Whitney *U* test.

rhage, or degenerated cell debris, which may produce varied appearances on CFP.[27]

Despite this potential variability, it is likely that the majority of SDOCT hyperreflective foci in intermediate AMD represents RPE cell migration. The authors observed that hyperreflectivity was almost always associated with drusen within the same ROI (96.6% of hyperreflectivity ROIs in Group B). This is consistent with previous observations that hyperpigmentation was frequently present around the center or rim of drusen, and in line with previous suggestions that hyperpigmentary lesions were due to the displacement or migration of RPE cells away from the apices of drusen.[16,28] Anderson et al.[17] proposed that cellular debris from compromised RPE cells, sequestered between the basal lamina and Bruch's membrane, contributes to drusenogenesis and generates a local proinflammatory signal. RPE cells migrate in the presence of TNF-α and TGF-β, suggesting that inflammatory mediators associated with drusen drive aberrant intraretinal RPE migration.[15,17,29,30] Although this hypothesis cannot be directly addressed without histopathologic correlation, the authors observed that intraretinal focal hyperreflectivity was most frequently localized to the inner aspect of drusen (Table 4). This supports the theory that drusen induce a loss of RPE structural integrity.[22,31,32] Inner migration of RPE cells into the retina will be identified better by future longitudinal studies corresponding intraretinal hyperreflectivity to hyperpigmentation over time.

Although the prevalence of drusen on CFP did not differ significantly between the ROI categories in Group A, the prevalence of RPE atrophy was significantly higher in the *hyperpigmentary* ROIs than *control* ROIs. However, in most regions with disagreement for RPE atrophy grading, the hypopigmented CFP areas were spatially correlated to small drusen on SDOCT and not RPE drop-out. This suggests that digital CFP grading may be limited in its ability to accurately distinguish RPE atrophy from small drusen, fibrosis, and other lesions.

A limitation of this study was possible bias in selecting the location of test regions. In Group A, *hyperpigmentary* and *control* ROIs differed significantly with respect to their distance from the fovea (Table 3). *Control* ROIs without hyperpigmentation were located further from the foveal center than *hyperpigmentary* ROIs. In Group B eyes, there was also a significant difference between *focal hyperreflectivity* and *control* ROIs with respect to their distance from the fovea (Table 3). This selection bias likely reflects the higher prevalence of AMD-associated pigmentary changes near the fovea. In order to avoid CFP pigmentation or SDOCT foci in the *control* ROIs, this study's masked graders may have found it necessary to select *control* ROIs further away from the foveal center.

In conclusion, this study has demonstrated a novel method of automated intermodality spatial correlation between CFP and SDOCT. With masked grading and automated spatial correspondence, CFP hyperpigmentary changes were often but not always correlated with the presence of focal SDOCT hyperreflective foci in eyes with intermediate AMD. Clinical phenotypes of AMD are currently based on fundus photograph criteria that were last defined in the 2003 AMD Phenotype Consensus Meeting sponsored by the National Eye Institute (http://www.nei.nih.gov/strategicplanning/amd_meeting.asp). With the findings of the AREDS2 Ancillary SDOCT Study, SDOCT imaging may help to define AMD stages with more accurate imaging markers. Additional longitudinal studies are warranted to investigate the association between CFP hyperpigmentation, correlated SDOCT lesions, and progression to advanced AMD. Improved characterization of pigmentary changes with SDOCT imaging may become clinically useful for AMD risk stratification, estimation of disease progression rate, and initiation of earlier pharmacologic intervention.

Acknowledgments

The authors thank Michelle McCall and Neeru Sarin for their assistance as AREDS2 Ancillary SDOCT Study coordinators.

References

1. Davis MD, Gangnon RE, Lee LY, et al. AREDS Research Group. The Age-Related Eye Disease Study severity scale for age-related macular degeneration: AREDS Report No. 17. *Arch Ophthalmol*. 2005;123:1484–1498.
2. Klein R, Klein BE, Linton KL. Prevalence of age-related maculopathy. The Beaver Dam Eye Study. *Ophthalmology*. 1992;99:933–943.
3. Vingerling JR, Dielemans I, Hofman A, et al. The prevalence of age-related maculopathy in the Rotterdam Study. *Ophthalmology*. 1995;102:205–210.
4. Augood CA, Vingerling JR, de Jong PT, et al. Prevalence of age-related maculopathy in older Europeans: the European Eye Study (EUREYE). *Arch Ophthalmol*. 2006;124:529–535.
5. Friedman DS, O'Colmain BJ, Munoz B, et al. Eye Diseases Prevalence Research Group. Prevalence of age-related macular degeneration in the United States. *Arch Ophthalmol*. 2004; 122:564–572.
6. Klaver CC, Wolfs RC, Vingerling JR, Hofman A, de Jong PT. Age-specific prevalence and causes of blindness and visual impairment in an older population: the Rotterdam Study. *Arch Ophthalmol*. 1998;116:653–658.
7. Klein R, Klein BE, Knudtson MD, Meuer SM, Swift M, Gangnon RE. Fifteen-year cumulative incidence of age-related macular degeneration: the Beaver Dam Eye Study. *Ophthalmology*. 2007;114:253–262.
8. Wang JJ, Rochtchina E, Lee AJ, et al. Ten-year incidence and progression of age-related maculopathy: the Blue Mountains Eye Study. *Ophthalmology*. 2007;114:92–98.
9. Klein ML, Ferris FL, Armstrong J, et al. AREDS Research Group. Retinal precursors and the development of geographic atrophy in age-related macular degeneration. *Ophthalmology*. 2008; 115:1026–1031.
10. Sunness JS, Margalit E, Srikumaran D, et al. The long-term natural history of geographic atrophy from age-related macular degeneration: enlargement of atrophy and implications for interventional clinical trials. *Ophthalmology*. 2007;114:271–277.
11. Van Leeuwen R, Klaver CC, Vingerling JR, Hofman A, de Jong PT. The risk and natural course of age-related maculopathy: follow-up at 6 1/2 years in the Rotterdam Study. *Arch Ophthalmol*. 2003;121:519–526.
12. Wang JJ, Foran S, Smith W, Mitchell P. Risk of age-related macular degeneration in eyes with macular drusen or hyperpigmentation: the Blue Mountains Eye Study cohort. *Arch Ophthalmol*. 2003;121:658–663.
13. Ferris FL, Davis MD, Clemons TE, et al. AREDS Research Group. A simplified severity scale for age-related macular degeneration: AREDS Report No. 18. *Arch Ophthalmol*. 2005; 123:1570–1574.
14. CAPT Research Group. Risk factors for choroidal neovascularization and geographic atrophy in the complications of age-related macular degeneration prevention trial. *Ophthalmology*. 2008;115:1474–1479.
15. Hageman GS, Mullins RF. Molecular composition of drusen as related to substructural phenotype. *Mol Vis*. 1999;5:28.
16. Pieroni CG, Witkin AJ, Ko TH, et al. Ultrahigh resolution optical coherence tomography in non-exudative age related macular degeneration. *Br J Ophthalmol*. 2006;90:191–197.

17. Anderson DH, Mullins RF, Hageman GS, Johnson LV. A role for local inflammation in the formation of drusen in the aging eye. *Am J Ophthalmol*. 2002;134:411–431.
18. Bearelly S, Chau FY, Koreishi A, Stinnett SS, Izatt JA, Toth CA. Spectral domain optical coherence tomography imaging of geographic atrophy margins. *Ophthalmology*. 2009;116:1762–1769.
19. Khanifar AA, Koreishi AF, Izatt JA, Toth CA. Drusen ultrastructure imaging with spectral domain optical coherence tomography in age-related macular degeneration. *Ophthalmology*. 2008;115:1883–1890.
20. Leuschen JN, Schuman SG, Winter KP, et al. Spectral domain optical coherence tomography characteristics of intermediate age-related macular degeneration. *Ophthalmology*. 2012. In press.
21. Jain N, Farsiu S, Khanifar AA, et al. Quantitative comparison of drusen segmented on SD-OCT versus drusen delineated on color fundus photographs. *Invest Ophthalmol Vis Sci*. 2010; 51:4875–4883.
22. Ho J, Witkin AJ, Liu J, et al. Documentation of intraretinal retinal pigment epithelium migration via high-speed ultrahigh-resolution optical coherence tomography. *Ophthalmology*. 2011;118:687–693.
23. Hubbard LD, Danis RP, Neider MW, et al. AREDS2 Research Group. Brightness, contrast, and color balance of digital versus film retinal images in the age-related eye disease study 2. *Invest Ophthalmol Vis Sci*. 2008;49:3269–3282.
24. AREDS Research Group. The Age-Related Eye Disease Study system for classifying age-related macular degeneration from stereoscopic color fundus photographs: AREDS Report No. 6. *Am J Ophthalmol*. 2001;132:668–681.
25. Chiu SJ, Izatt JA, O'Connell RV, Winter KP, Toth CA, Farsiu S. Validated automatic segmentation of AMD pathology including drusen and geographic atrophy in SDOCT images. *Invest Ophthalmol Vis Sci*. 2012;53:53–61.
26. Chiu SJ, Li XT, Nicholas P, Toth CA, Izatt JA, Farsiu S. Automatic segmentation of seven retinal layers in SDOCT images congruent with expert manual segmentation. *Opt Express*. 2010;18:19413–19428.
27. Schuman SG, Koreishi AF, Farsiu S, Jung SH, Izatt JA, Toth CA. Photoreceptor layer thinning over drusen in eyes with age-related macular degeneration imaged in vivo with spectral-domain optical coherence tomography. *Ophthalmology*. 2009; 116:488–496.
28. Zacks DN, Johnson MW. Transretinal pigment migration: an optical coherence tomography study. *Arch Ophthalmol*. 2004; 122:406–407.
29. Jin M, He S, Worpel V, Ryan SJ, Hinton DR. Promotion of adhesion and migration of RPE cells to provisional extracellular matrices by TNF-alpha. *Invest Ophthalmol Vis Sci*. 2000; 41:4324–4332.
30. Mitsuhiro MR, Eguchi S, Yamashita H. Regulation mechanisms of retinal pigment epithelial cell migration by the TGF-beta superfamily. *Acta Ophthalmol Scand*. 2003;81:630–638.
31. Ma W, Zhao L, Fontainhas AM, Fariss RN, Wong WT. Microglia in the mouse retina alter the structure and function of retinal pigmented epithelial cells: a potential cellular interaction relevant to AMD. *PLoS One*. 2009;4:e7945.
32. Cukras C, Agron E, Klein ML, et al. AREDS Research Group. Natural history of drusenoid pigment epithelial detachment in age-related macular degeneration: AREDS Report No. 28. *Ophthalmology*. 2010;117:489–499.